
LEARNING SPARSE INTERACTION GRAPHS OF PARTIALLY OBSERVED PEDESTRIANS FOR TRAJECTORY PREDICTION

Zhe Huang

University of Illinois at Urbana-Champaign
zheh4@illinois.edu

Ruohua Li

University of Michigan
ruohuali@umich.edu

Kazuki Shin

University of Illinois at Urbana-Champaign
kazukis2@illinois.edu

Katherine Driggs-Campbell

University of Illinois at Urbana-Champaign
krdc@illinois.edu

ABSTRACT

Multi-pedestrian trajectory prediction is an indispensable safety element of autonomous systems that interact with crowds in unstructured environments. Many recent efforts have developed trajectory prediction algorithms with focus on understanding social norms behind pedestrian motions. Yet we observe these works usually hold two assumptions that prevent them from being smoothly applied to robot applications: positions of all pedestrians are consistently tracked; the target agent pays attention to all pedestrians in the scene. The first assumption leads to biased interaction modeling with incomplete pedestrian data, and the second assumption introduces unnecessary disturbances and leads to the freezing robot problem. Thus, we propose Gumbel Social Transformer, in which an Edge Gumbel Selector samples a sparse interaction graph of partially observed pedestrians at each time step. A Node Transformer Encoder and a Masked LSTM encode the pedestrian features with the sampled sparse graphs to predict trajectories. We demonstrate that our model overcomes the potential problems caused by the assumptions, and our approach outperforms the related works in benchmark evaluation.

Keywords Human-Centered Autonomy, Pedestrian Trajectory Prediction, Graph Structure Learning

1 Introduction

A comprehensive understanding of dynamic human environments is essential for autonomous mobile robots to safely and smoothly enter our daily lives [Chen et al., 2017]. The mobile robot needs to effectively encode motion patterns of surrounding pedestrians from observation data, accurately predict their future trajectories, and efficiently plan its own paths for rapid task execution free of safety risks [Ziebart et al., 2009, Du et al., 2020]. Social awareness is crucial for robots to achieve such human-centered autonomy, and significant progress has been made to acquire this capability by studying human-human interaction and predicting trajectories of multiple pedestrians [Alahi et al., 2016, Vemula et al., 2018, Gupta et al., 2018, Ivanovic and Pavone, 2019, Zhang et al., 2019]. These interactive models inspired new contributions in multi-agent motion planning and crowd navigation [Chen et al., 2019, Liu et al., 2021].

Despite the fruitful results on building socially aware architectures for multi-pedestrian trajectory prediction, previous works usually hold two assumptions which may burden their robotic applications in the real world. The first assumption is positions of all pedestrians are successfully tracked at all times. The second assumption is the target agent (pedestrian or robot) pays attention to all pedestrians in the considered public scene regardless of the size of space [Gupta et al., 2018].

The first assumption requires that only the pedestrians who are fully observed are considered for modeling social interaction and predicting trajectories in future. However, in reality pedestrians enter and exit the considered scene or the detection range of the robot at different times. Therefore, a number of detected pedestrians are partially observed,

which means they are tracked during a period but may not be fully observed. Although this eases model implementation and evaluation, we find the first assumption results in 40.7% pedestrians in benchmark datasets ignored due to partial observability. Moreover, incomplete pedestrian data leads to biased modeling on social interactions. The second assumption allows pedestrians that are clearly non-influential (e.g. being far away from the target agent with many other pedestrians in-between) to affect motion of the target agent. A workaround to the second assumption is that the target agent needs to pay attention to all pedestrians in a pre-defined neighborhood, in order to exclude the distant and insignificant ones, but the joint influence from too many neighbors in close proximity would still potentially impair the path planning of the target agent, and cause the notorious freezing robot problem [Trautman and Krause, 2010].

We propose Gumbel Social Transformer, which is composed of Edge Gumbel Selector, Node Transformer Encoder, and Masked LSTM. Each component is designed to be capable of processing features of partially observed pedestrians in order to handle the first assumption. As for the second assumption, we formulate a directed interaction graph to represent relationships over partially observed pedestrians at each time step. In the interaction graph, a node represents a pedestrian, and a directed edge represents a connection that the node at its tail pays attention to the node at its head. The graph is initiated with full connection which is equivalent as attention to all pedestrians mentioned in the second assumption. We apply the Edge Gumbel Selector to prune the edges by following an important constraint: *The target agent can pay attention to at most n pedestrians*. The hyperparameter n is to control the graph sparsity. With the most important relationships preserved between each agent and its n neighbors at each time step, the sparse interaction graphs inferred by the Edge Gumbel Selector are stacked in sequence. The sequence is then fed into the Node Transformer Encoder and the Masked LSTM to spatially and temporally encode features of partially observed pedestrians, and recursively predict their trajectories.

Our contributions are fourfold: (1) We present a novel architecture to predict trajectories of partially observed pedestrians; (2) We introduce an Edge Gumbel Selector to sample dynamic and sparse interaction graphs of partially observed pedestrians; (3) We demonstrate in multi-agent simulation that our model mitigates the freezing robot problem and diminishes the disturbance from non-influential neighbors on the target agent; and (4) Our model outperforms state-of-the-art approaches on public human trajectory datasets.

2 Related Work

Pedestrian Trajectory Prediction. Early works exhaustively investigated hand-engineered features of pedestrian motion [Helbing and Molnar, 1995, Van den Berg et al., 2008]. These works perform well in certain cases, but have non-negligible limitations, such as failed generalization to different scenarios and fixed motion patterns across all pedestrians [Ferrer and Sanfeliu, 2014]. Substantial contributions were made to resolve these problems by the integration of socially-aware structures and deep learning methods, including Social LSTM [Alahi et al., 2016], Generative Adversarial Networks [Gupta et al., 2018], Self-Attention Mechanism [Vemula et al., 2018, Zhang et al., 2019], Graph Neural Networks [Huang et al., 2019, Mohamed et al., 2020], and Transformer [Yu et al., 2020]. The assumptions of fully observed pedestrians and global attention over the whole scene are enforced in many previous works [Vemula et al., 2018, Gupta et al., 2018, Huang et al., 2019, Mohamed et al., 2020, Yu et al., 2020], whereas others constrained the target agent to pay attention within a small neighborhood region, or did not clarify how motion prediction on fully observed pedestrians would be affected by considering partially observed pedestrians [Alahi et al., 2016, Zhang et al., 2019]. In contrast to these existing works, our work infers a sparse interaction graph among pedestrians in an unsupervised manner, and explicitly studies the influence of partially observed pedestrians on pedestrian trajectory prediction.

Graph Structure Learning. Graph generation has a wide range of applications, including but not limited to causal discovery [Zhu et al., 2019], neural architecture search [Xie et al., 2019], molecule design [Jin et al., 2018], and physical interaction inference [Kipf et al., 2018]. Traditional approaches were typically hand-crafted for a specific family of graphs [Erdős and Rényi, 1960], whereas the power of deep learning on modeling complex domains was recently harnessed to learn graphs with suitable properties from observed data. One choice is to use Recurrent Neural Networks and perform sequential prediction on the next node or edge to be added to the graph [You et al., 2018], while another choice is to generate adjacency matrix in one shot when the number of graph nodes is fixed [Anand and Huang, 2018]. Dropout on the adjacency matrix (i.e., dropout on edges) is often used to alleviate over-fitting and over-smoothing issues [Vaswani et al., 2017, Rong et al., 2019]. Besides regularization, graph sparsity is usually emphasized in many domains, where sparse graph representations are necessary to learn model parameters more efficiently [Xie et al., 2019, Kipf et al., 2018]. Probability distribution of edges are usually assumed independent Bernoulli variables (existence of a single edge) [Franceschi et al., 2019] or independent categorical variables (type of a single edge) [Kipf et al., 2018, Li et al., 2019]. In addition, previous works which are focused on dynamical systems assume the graph structure is unchanged over time [Kipf et al., 2018, Li et al., 2019]. In our work, we consider the categorical distribution *over* edges connecting neighbor pedestrian nodes to the same target node, and the inferred graph structure can change dynamically.

3 Method

3.1 Problem Formulation

Consider N pedestrians who appear in a street scene in an observation period $t \in \{1, \dots, T_{obs}\}$. Their 2D positions are denoted by x_i^t , $i \in \{1, \dots, N\}$. The task is to jointly predict their trajectories x_i^t in a prediction period $t \in \{T_{obs} + 1, \dots, T_{obs} + T_{pred}\}$. Fully observed pedestrians show up at each time step during the whole observation and prediction period, while partially observed pedestrians may either enter the scene later than $t = 1$ or leave the scene earlier than $t = T_{obs} + T_{pred}$. We assume all pedestrian trajectories are continuous with no misdetection¹.

We introduce *interaction graphs* to represent motion of partially observed pedestrians. A directed interaction graph $G^t = (V^t, E^t, M^t, A^t)$ describes pedestrian motion at a time step t . The set of nodes $V^t = \{v_i^t\}_{i=1:N}$ corresponds to pedestrian displacement (i.e., velocity), and the set of edges $E^t = \{e_{ij}^t\}_{i,j=1:N}$ correspond to the relative position from a target pedestrian i to a neighbor j . The node masks $M^t = \{m_i^t\}_{i=1:N}$ indicate whether the i th pedestrian’s position is recorded at both $t - 1$ and t , and the binary-valued adjacency matrix $A^t = \{a_{ij}^t\}_{i,j=1:N}$ specifies the validity of edges as in Equation 1, where the edge e_{ij}^t is nonexistent whenever either v_i^t or v_j^t is invalid. This setting guarantees the full connectivity of G^t by removing the node of a pedestrian, who has not shown up yet or has left the scene, and removing all edges relevant to that node. The linear embedding layers and the masks for nodes and edges are applied to respective attributes to obtain high dimensional features, which are still denoted by v_i^t and e_{ij}^t as in Equation 2. Note global positions are not explicitly used to extract node features, as the potential coordinate shift issue could weaken generalization across different scenes [Huang et al., 2019, 2021].

$$m_i^t = \mathbb{1} \{x_i^{t-1} \text{ and } x_i^t \text{ are valid}\}, \quad a_{ij}^t = m_i^t m_j^t \quad (1)$$

$$v_i^t = m_i^t \phi_v(x_i^t - x_i^{t-1}), \quad e_{ij}^t = a_{ij}^t \phi_e(x_j^t - x_i^t) \quad (2)$$

3.2 Gumbel Social Transformer

The architecture of the Gumbel Social Transformer is illustrated in Figure 1. An Edge Gumbel Selector takes as input a combination of node and edge representations from Interaction Graph Representations, and samples a sparse interaction graph at each observation time step. A Node Transformer Encoder spatially aggregates node representations of the sampled sparse interaction graphs. The spatially encoded node features are sequentially fed into a Masked LSTM, where the hidden states are used to predict pedestrian positions at the next step. The recursion of feature embedding, edge sampling, node encoding, and node decoding is repeated until the end of prediction period.

Edge Gumbel Selector. Though the interaction graph G^t includes complete details of the pedestrian motion at the moment, full connectivity could be redundant, and even adversely affect the modeling of a target pedestrian i ’s behavior. We impose the n -neighbor sparsity constraint on the interaction graph, which leads to a sparse interaction graph $\tilde{G}^t = (\tilde{V}^t, \tilde{E}^t, \tilde{M}^t, \tilde{A}^t)$. While $\tilde{V}^t, \tilde{E}^t, \tilde{M}^t$ are identical to the counterparts in G^t , the weighted adjacency matrix $\tilde{A}^t = \{\tilde{a}_{ij}^t\}_{i,j=1:N} \in [0, 1]^{N \times N}$ becomes a sparse float-valued matrix to be inferred.

The inference of the adjacency matrix \tilde{A}^t is formulated as the problem to find the n neighbors that has the most influence on a target pedestrian i . We first concatenate neighbor node features, target node features, and edge features to obtain augmented edge features \hat{e}_{ij}^t , which represent the pairwise interaction between target i and a neighbor j . A neighbor may draw the attention from the target that was originally paid to another neighbor. The relationship of these pairwise interactions \hat{e}_{ij}^t themselves is captured by a multi-head attention (MHA) at the edge level. The number of heads is set as n , where each head can be interpreted as one type of the interaction relationship:

$$\hat{e}_{ij}^t = [v_j^t \| v_i^t \| e_{ij}^t], \quad \{\hat{e}_{ij}^{t,k}\}_{j=1:N}^{k=1:n} = \text{MHA}(Q, K, V = \{\hat{e}_{ij}^t\}_{j=1:N}, \text{mask} = \{a_{ij}^t\}_{j=1:N}) \quad (3)$$

A multi-layer perceptron (MLP) maps the aggregated augmented edge features $\hat{e}_{ij}^{t,k}$ to log probabilities $\alpha_{ij}^{t,k}$ of a N -dimensional categorical distribution corresponding to the k th head. A reparameterization trick named Gumbel Softmax [Jang et al., 2017] is used to sample the most important neighbor to the i th target from these categorical distributions at each head while preserving differentiability. The samples are drawn from the concrete distribution

¹This assumption requires decent tracking performance of the robot, but relaxes the condition on pedestrians so they can come in and out of the detection range at any time.

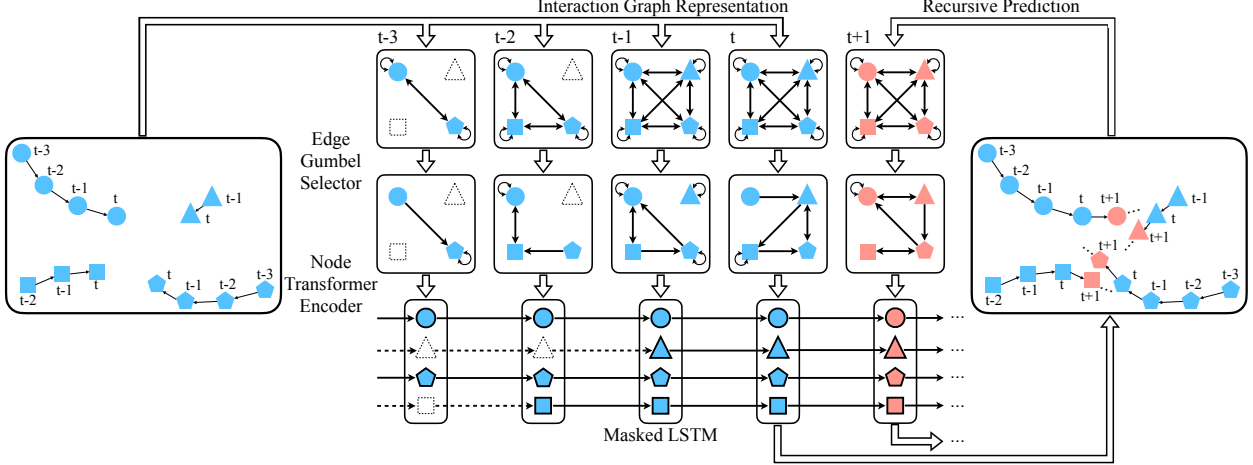


Figure 1: Overview of Gumbel Social Transformer. Observed trajectories (blue) are processed into Interaction Graph Representations which are fully connected except for unobserved pedestrian nodes. Edge Gumbel Selector samples the interaction graph under the sparsity constraint, which are encoded by Node Transformer Encoder and Masked LSTM. The encoded pedestrian features are used to recursively predict trajectories (red).

approximation [Maddison et al., 2017] as presented in Equation 4, where $\mathbf{g} \in \mathbb{R}^N$ is a vector with elements sampled from independent and identically distributed random variables with Gumbel(0, 1) distribution.

$$\alpha_{ij}^{t,k} = \text{MLP}(\hat{e}_{ij}^{t,k}), \quad \tilde{a}_{ij}^{t,k} = \text{softmax}_j \left(\left(\alpha_{ij}^{t,k} + \mathbf{g} \right) / \tau \right), \quad \tilde{a}_{ij}^t = \frac{1}{n} \sum_k \tilde{a}_{ij}^{t,k} \quad (4)$$

The temperature hyperparameter τ in Equation 4 is annealed to near zero during the training process, so that the approximate samples gradually converge to one-hot samples from the categorical distributions. The entries of the sampled weighted adjacency matrix \tilde{a}_{ij}^t 's are the mean of generated samples across the heads. Note that the sampling process assures that the set of invalid edges in \tilde{E}^t is a subset of the set of the removed edges in \tilde{A}^t .

Node Transformer Encoder. Given the sparse interaction graph \tilde{G}^t , the node features are spatially aggregated using an encoder inspired by Transformer-based Graph Convolution (TGConv) [Yu et al., 2020]. The main difference is that TGConv is equivalent as applying to Transformer a binary attention mask representing the connection of pedestrians, which is an all-one square matrix in previous work due to the assumptions of fully connected graph and fully observed pedestrians [Yu et al., 2020]. The Node Transformer Encoder in our case takes the weighted adjacency matrix \tilde{A}^t as the attention mask, which is a sparse and float matrix, and the inputs of source and target sequences² of Transformer are the representations of partially observed pedestrians \tilde{V}^t . More details of TGConv and its variant used for Node Transformer Encoder are attached to the supplementary material.

$$\{\hat{v}_i^t\}_{i=1:N} = \text{TGConv}(\text{target} = \tilde{V}^t, \text{source} = \tilde{V}^t, \text{mask} = \tilde{A}^t) \quad (5)$$

Masked LSTM. Pedestrian motion during observation period is sliced into a stack of interaction graphs $\{G^t\}_{t=1:T_{obs}}$, which are processed through the Edge Gumbel Selector and the Node Transformer Encoder to obtain spatially encoded node features $\{\hat{v}_i^t\}_{i=1:N}^{t=1:T_{obs}}$. Then the node features are sequentially fed into a Masked LSTM to propagate hidden features, which are used to predict pedestrian positions through a linear layer. The node masks m_i^t 's are set as one through prediction period for all pedestrians except for who disappear before or at T_{obs} , since they will never come back into the scene as assumed in Section 3.1. The recurrence is introduced by generating the Interaction Graph Representation at the next step with the predicted positions.

$$h_i^{t+1} = (1 - m_i^t) h_i^t + m_i^t \text{LSTM}(\hat{v}_i^t, h_i^t), \quad \hat{x}_i^{t+1} = \hat{x}_i^t + \phi_h(h_i^{t+1}) \quad (6)$$

²The word ‘‘sequence’’ follows the language of Transformer, but ‘‘set’’ may be a better word than ‘‘sequence’’ in the pedestrian context.

4 Experiments

We use two publicly available trajectory datasets for benchmarking: ETH [Pellegrini et al., 2009] and UCY [Lerner et al., 2007]. ETH is composed of two scenes ETH and HOTEL, and UCY is composed of three scenes UNIV, ZARA1, and ZARA2. The frame rate is 2.5 frames per second and is consistent across the scenes. The task is to predict the trajectories in the next 4.8 seconds ($T_{pred} = 12$) given the positions tracked in the latest 3.2 seconds ($T_{obs} = 8$). Trajectory samples in each scene are split into the training set (80%) and the test set (20%), and models are independently trained for each scene. Additionally, we conduct comparative study on our models trained with various configurations by analyzing their performance in synthesized scenarios of multi-agent simulation.

4.1 Implementation Details

The embedding dimension of nodes is 32 and of edges is 64. The dimension of hidden states in LSTM is 32. The temperature τ of the Edge Gumbel Selector is annealed linearly from 0.5 to 0.03 through the training process. The Node Transformer Encoder has three Transformer Encoder layers with 8 attention heads, and a feed-forward dimension of 128. The Adam optimizer is used to minimize the mean square error loss of prediction on trajectories of partially observed pedestrians [Kingma and Ba, 2015], with initial learning rate of 0.001. For each scene, the model is trained for 200 epochs. The trajectory samples are randomly rotated during the training process for data augmentation.

4.2 Benchmark Evaluation

Baselines. Our model is compared against several existing methods: (1) Social LSTM (SLSTM-D) is a LSTM integrated with a social pooling layer that outputs deterministic trajectories [Alahi et al., 2016]; (2) Social STGCNN (STGCN) is a spatial graph convolution network concatenated with a temporal convolution network that generates probabilistic outputs [Mohamed et al., 2020]; (3) STGCN-D is the variant of STGCN that generates deterministic prediction; (4) Social GAN (SGAN) has a LSTM-based encoder-decoder architecture with a socially aware global pooling layer, and is trained using Generative Adversarial Networks for multi-modal trajectory prediction [Gupta et al., 2018]; (5) Spatial-Temporal GAT (STGAT) applies graph attention networks to model crowd interaction, and uses different LSTMs for temporal encoding of individual pedestrians and of spatially encoded interaction [Huang et al., 2019].

Metrics. Offset Error is used to evaluate prediction performance, which is defined as the distance between the target pedestrian’s ground truth position and the position predicted by the model at one time step [Alahi et al., 2016, Huang et al., 2021]. Average Offset Error (AOE) is the average of Offset Errors throughout the prediction period, and Final Offset Error (FOE) is the Offset Error at the last prediction step $T_{obs} + T_{pred}$. For evaluation of probabilistic methods, 20 trajectories in prediction period are generated, over which the mean and the standard deviation of AOE and FOEs are reported.

Table 1: Quantitative performance of all approaches on benchmark datasets. Two metrics Average Offset Error (AOE) and Final Offset Error (FOE) on fully observed pedestrians are reported (unit: m). The index of Gumbel Social Transformer (GST) corresponds to the ID in Table 2.

Metric	Method	ETH	HOTEL	UNIV	ZARA1	ZARA2	AVG
AOE ↓	SLSTM-D	2.45±0.00	0.81±0.00	1.24±0.00	2.48±0.00	1.07±0.00	1.61±0.00
	STGCN	2.93±0.59	1.07±0.21	0.76±0.05	0.95±0.23	0.87±0.14	1.32±0.25
	STGCN-D	2.67±0.00	0.74±0.00	0.64±0.00	0.68±0.00	0.59±0.00	1.06±0.00
	SGAN	1.78±0.55	0.32±0.08	0.62±0.03	0.59±0.11	0.43±0.10	0.75±0.17
	STGAT	1.51±0.68	0.26±0.09	0.57±0.08	0.52±0.19	0.45±0.16	0.66±0.24
	GST ₈	0.96±0.20	0.23±0.03	0.51±0.00	0.40±0.00	0.32±0.02	0.48±0.05
FOE ↓	SLSTM-D	4.20±0.00	1.46±0.00	2.20±0.00	4.49±0.00	1.93±0.00	2.86±0.00
	STGCN	4.98±0.89	1.54±0.29	1.39±0.09	1.48±0.30	1.31±0.20	2.14±0.35
	STGCN-D	4.83±0.00	1.23±0.00	1.26±0.00	1.28±0.00	1.06±0.00	1.93±0.00
	SGAN	3.60±1.33	0.60±0.19	1.31±0.06	1.28±0.26	0.94±0.21	1.55±0.41
	STGAT	3.01±1.41	0.48±0.21	1.23±0.18	1.15±0.46	1.02±0.42	1.38±0.54
	GST ₈	2.09±0.47	0.42±0.05	1.11±0.00	0.86±0.00	0.71±0.04	1.04±0.11

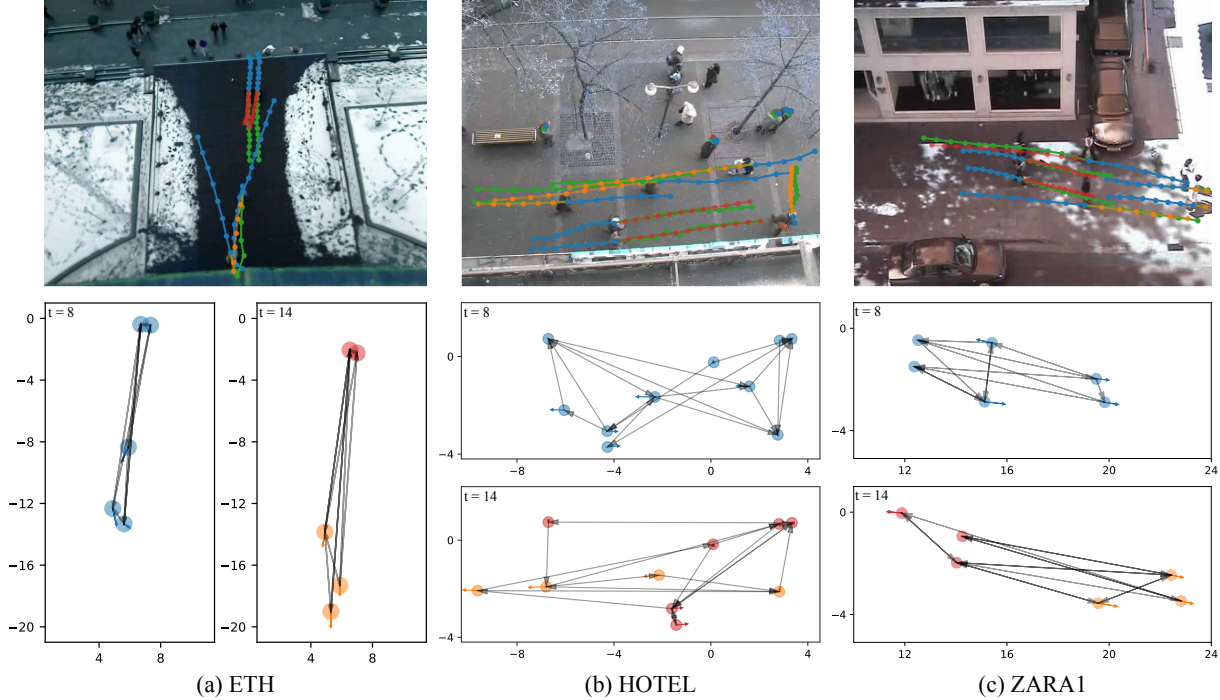


Figure 2: Trajectory prediction and sparse interaction graph inference on benchmark datasets. Blue denotes observation, green denotes ground truth, red denotes prediction on fully observed pedestrians, and orange denotes prediction on other partially observed pedestrians. Colored arrows indicate pedestrian velocities. Gray arrows represent directed edges of the interaction graph, where the target pedestrian node at the tail pays attention to the neighbor node at the head.

Results. The quantitative results are presented in Table 1. Note that our model GST is trained with partially observed pedestrians, while other baselines have to be trained with only fully observed pedestrians. Nevertheless, AOE and FOE are only reported on fully observed pedestrians for fair comparison across the methods. Our model GST exceeds the performance of other state-of-the-art approaches, and has a lower variance on the results compared to the baselines. The stochasticity of STGCN comes from the Gaussian displacement outputs, while SGAN and STGAT manipulate pedestrian motion patterns by concatenation of latent representations and random noise. In contrast, the probabilistic nature of our model is due to sampling of sparse interaction graphs, which has an implicit effect on trajectory prediction.

Visualization. Trajectory prediction and the inferred sparse interaction graphs on different scenes are visualized in Figure 2. Our model is able to predict the trajectories of those partially observed pedestrians, and also model their interaction with fully observed pedestrians by inferring the sparse interaction graphs. We visualize these graphs at $t=8$ and $t=14$ in each scene, where the former is the last observed time step, and the latter is at the middle of the prediction period. The graph structure varies at different times, indicating the evolution of the relationship between pedestrians during the change of their positions and velocities. In the HOTEL scene, two fully observed pedestrians at bottom were considered not interactive at $t=8$, while the mutual attention is built later at $t=14$ during the recursive prediction. On the contrary, there were initially bi-directed edges between the two pedestrian nodes in the middle of the ZARA1 scene at $t=8$. However, they walked away from each other, and both edges are removed at $t=14$. As presented in Figure 2, there exist edges that connect pedestrians who seem too far apart. While seemingly counterintuitive, we argue that it is reasonable for the target agent to pay attention to some distant neighbors for a small amount of time. Similar to a human pedestrian glancing over surrounding environments for efficient anomaly check (e.g. fast-moving skateboarders), the sparse and dynamic interaction graphs may lower the collision risk in the near future, by enabling the target agent to acknowledge the distant individuals while preventing too much attention drawn from them.

4.3 Comparative Study

The effect that each component of Gumbel Social Transformer has on the performance of trajectory prediction is assessed by extensive experiments with various configurations. Moreover, we apply our models to generate trajectories of multiple agents in simulation, and investigate their capabilities to tackle the common yet nontrivial scenarios in practical robot applications. The scenarios include (1) human agents join in the scene at different times; (2) one robot

agent meets a crowd of human agents; and (3) non-influential human agents walk randomly without purposes in the scene³.

Partially or Fully Observed Pedestrians. Though we only evaluate AOE and FOE on fully observed pedestrians, we see significant improvements by encoding the motion of fully observed pedestrians with other partially observed pedestrians. Table 2 shows 11.0/7.8% improvement on AOE/FOE when the model takes as input partially observed pedestrians over the fully observed ones. The trajectories of partially observed pedestrians create a complete picture of pedestrian interaction during the observation period, and thus provides an unbiased input for encoding socially aware pedestrian features. The importance of partially observed pedestrians is illustrated in Figure 3 (a), where a robot agent and a fully observed human agent walk against each other. The second human agent appears 1.6 seconds (4 time steps) later and starts approaching other agents. The top of Figure 3 (a) shows the case when both the robot and the fully observed human ignore the partially observed one. In contrast, the bottom of Figure 3 (a) illustrates that both agents deviate from the original path to dodge the partially observed human.

Sparse or Fully Connected Interaction Graph. Imposing sparsity on the graph structure does not greatly influence the quantitative performance unless the requirement of taking partially observed pedestrians as input is satisfied. Table 2 shows the sparse configuration GST₈ improves AOE/FOE by 8.0/6.1% compared to the fully connected configuration GST₅ under the partially observed pedestrian setting. However, the same configurations under the setting of fully observed pedestrians GST₄ and GST₁ have comparable performance. The intuition behind this result is that the most important pedestrian that requires attention may not be fully observed. Including this agent in the input data by considering partially observed pedestrians is the premise of successfully sampling the connection with this agent during the edge selection process. Besides the quantitative improvements, sparsity is critical to deal with the freezing robot situation. As shown in Figure 3 (b), a robot agent is moving right and encounters a human crowd of eight moving left. The top of Figure 3 (b) presents the results of GST₅ where Edge Gumbel Selector is disabled, from which we see the robot agent turned around in order to dodge the crowd. We reason that the single robot agent has to consider all people in the crowd, and features from the crowd overwhelmed its own features in the weighted sum step of self-attention. The U-turn behavior happens, because all the members in the crowd jointly *push back* the single agent against its own will through the forward pass on the fully connected interaction graph. As shown on the bottom of Figure 3 (b), this unnatural turnaround motion is effectively alleviated by enabling Edge Gumbel selector to introduce sparsity (GST₈). The robot agent interacts with the most important neighbors in the crowd, and avoid collisions while actively moving to the right. In addition to the freezing robot issue, note that the trajectories predicted for the agents in the crowd are trivially identical on the top of Figure 3 (b). This is because node features of the human agents are the same by processing the same observed displacements, while the fully connected graph structure preserves the symmetry of aggregated node features which results in the exactly same motions.

The Level of Sparsity. The sparsity of the interaction graph is controlled by n , which is the upper bound of number of pedestrians that one can pay attention to in the scene. This hyperparameter is set as 1, 4 and 16 in our comparative study, and we find in general $n=1$ obtains the best quantitative performance. Besides improving the quantitative performance, control of the sparsity level is necessary to help target agent concentrate on interaction with the critical neighbors. Figure 3 (c) illustrates a scene where six human agents are moving randomly near the boundaries, and an important human agent is running into the robot. The top of Figure 3 (c) shows the results with $n=16$, where the robot and the

Table 2: Comparative study on Gumbel Social Transformer. Partial denotes whether partially observed pedestrians are taken as input. Sparsity denotes whether we apply Edge Gumbel Selector for sampling sparse interaction graphs. The hyperparameter n is the upper bound on the number of pedestrians to whom a target agent can pay attention.

ID	Partial	Sparsity	n	AOE ↓	FOE ↓
1	-	-	N/A	0.59±0.00	1.18±0.00
2	-	✓	16	0.57±0.03	1.20±0.06
3	-	✓	4	0.59±0.02	1.25±0.05
4	-	✓	1	0.58±0.01	1.20±0.02
5	✓	-	N/A	0.52±0.00	1.11±0.00
6	✓	✓	16	0.53±0.03	1.14±0.07
7	✓	✓	4	0.54±0.05	1.17±0.11
8	✓	✓	1	0.48±0.05	1.04±0.11

³Human and robot are treated as equivalent agents, which follows the setup of the crowd navigation simulation in [Chen et al., 2019].

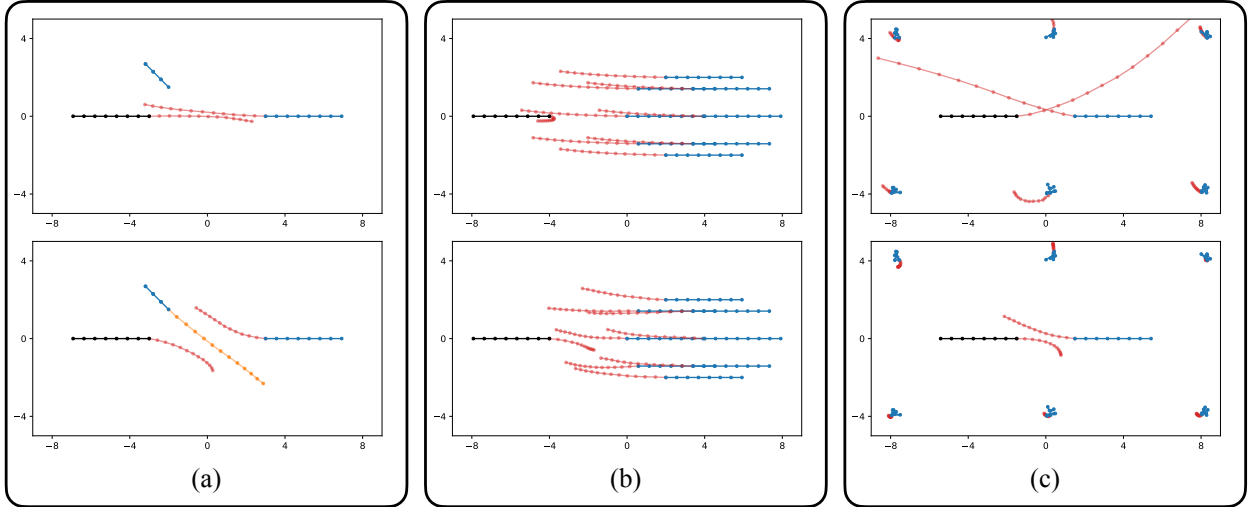


Figure 3: Comparison of multi-agent simulation results in different human-robot interaction scenarios: (a) Human agents enter the robot agent’s field of view at different times; (b) One robot agent encounters a group of human agents; (c) Some human agents walk aimlessly in the scene. Black and blue represents the observation on robot and human agents. Red indicates prediction on the robot and fully observed pedestrians, and orange indicates prediction on partially observed pedestrians.

interactive human exhibit exaggerated high-speed motion. In comparison, the robot agent avoids the collision with the close human neighbor naturally in the bottom of Figure 3 (c), which illustrates the results with $n=4$. This indicates that when the interaction graph is close to fully connected, the target agent is easy to be affected by the connected neighbors, even the ones who are clearly non-influential.

5 Conclusions

We identify two common assumptions of existing pedestrian trajectory prediction approaches: pedestrian positions are always successfully tracked and observed, and the target agent pays attention to all pedestrians in the detected range. The assumptions can cause potential limitations on the deployment of trajectory prediction algorithms onto the real world robot applications. We present Gumbel Social Transformer to overcome these limitations. Our model architecture is designed to encode features of partially observed pedestrians, and thus provides a complete input for unbiased modeling on pedestrian interaction. We propose Edge Gumbel Selector, which is an unsupervised method, to infer a sequence of sparse interaction graphs that summarize the evolving relationship among pedestrians. We demonstrate the introduction of sparsity into modeling multi-agent interaction effectively alleviates the freezing robot problem, and minimizes the influence on generating target agent’s motion from unimportant neighbors. In the future, we would integrate our socially aware trajectory prediction model with motion planning algorithms, and implement robot navigation through dense crowds in public scenes.

References

- Yu Fan Chen, Michael Everett, Miao Liu, and Jonathan P How. Socially aware motion planning with deep reinforcement learning. In *Proceedings of the IEEE/RSJ International Conference on Intelligent Robots and Systems*, pages 1343–1350, 2017.
- Brian D Ziebart, Nathan Ratliff, Garratt Gallagher, Christoph Mertz, Kevin Peterson, J Andrew Bagnell, Martial Hebert, Anind K Dey, and Siddhartha Srinivasa. Planning-based prediction for pedestrians. In *Proceedings of the IEEE/RSJ International Conference on Intelligent Robots and Systems*, pages 3931–3936, 2009.
- Peter Du, Zhe Huang, Tianqi Liu, Ke Xu, Qichao Gao, Hussein Sibai, Katherine Driggs-Campbell, and Sayan Mitra. Online monitoring for safe pedestrian-vehicle interactions. In *Proceedings of the IEEE International Conference on Intelligent Transportation Systems*, 2020.

- Alexandre Alahi, Kratarth Goel, Vignesh Ramanathan, Alexandre Robicquet, Li Fei-Fei, and Silvio Savarese. Social lstm: Human trajectory prediction in crowded spaces. In *Proceedings of the IEEE/CVF Conference on Computer Vision and Pattern Recognition*, pages 961–971, 2016.
- Anirudh Vemula, Katharina Muelling, and Jean Oh. Social attention: Modeling attention in human crowds. In *Proceedings of the IEEE International Conference on Robotics and Automation*, pages 4601–4607, 2018.
- Agrim Gupta, Justin Johnson, Li Fei-Fei, Silvio Savarese, and Alexandre Alahi. Social gan: Socially acceptable trajectories with generative adversarial networks. In *Proceedings of the IEEE/CVF Conference on Computer Vision and Pattern Recognition*, pages 2255–2264, 2018.
- Boris Ivanovic and Marco Pavone. The trajectron: Probabilistic multi-agent trajectory modeling with dynamic spatiotemporal graphs. In *Proceedings of the IEEE/CVF International Conference on Computer Vision*, pages 2375–2384, 2019.
- Pu Zhang, Wanli Ouyang, Pengfei Zhang, Jianru Xue, and Nanning Zheng. Sr-lstm: State refinement for lstm towards pedestrian trajectory prediction. In *Proceedings of the IEEE/CVF Conference on Computer Vision and Pattern Recognition*, pages 12085–12094, 2019.
- Changan Chen, Yuejiang Liu, Sven Kreiss, and Alexandre Alahi. Crowd-robot interaction: Crowd-aware robot navigation with attention-based deep reinforcement learning. In *Proceedings of the IEEE International Conference on Robotics and Automation*, pages 6015–6022, 2019.
- Shuijing Liu, Peixin Chang, Weihang Liang, Neeloy Chakraborty, and Katherine Driggs-Campbell. Decentralized structural-rnn for robot crowd navigation with deep reinforcement learning. In *Proceedings of the IEEE International Conference on Robotics and Automation*, 2021.
- Peter Trautman and Andreas Krause. Unfreezing the robot: Navigation in dense, interacting crowds. In *Proceedings of the IEEE/RSJ International Conference on Intelligent Robots and Systems*, pages 797–803, 2010.
- Dirk Helbing and Peter Molnar. Social force model for pedestrian dynamics. *Physical review E*, 51(5):4282, 1995.
- Jur Van den Berg, Ming Lin, and Dinesh Manocha. Reciprocal velocity obstacles for real-time multi-agent navigation. In *Proceedings of the IEEE International Conference on Robotics and Automation*, pages 1928–1935, 2008.
- Gonzalo Ferrer and Alberto Sanfeliu. Behavior estimation for a complete framework for human motion prediction in crowded environments. In *Proceedings of the IEEE International Conference on Robotics and Automation*, pages 5940–5945. IEEE, 2014.
- Yingfan Huang, Huikun Bi, Zhaoxin Li, Tianlu Mao, and Zhaoqi Wang. Stgat: Modeling spatial-temporal interactions for human trajectory prediction. In *Proceedings of the IEEE/CVF International Conference on Computer Vision*, pages 6272–6281, 2019.
- Abduallah Mohamed, Kun Qian, Mohamed Elhoseiny, and Christian Claudel. Social-stgcnn: A social spatio-temporal graph convolutional neural network for human trajectory prediction. In *Proceedings of the IEEE/CVF Conference on Computer Vision and Pattern Recognition*, 2020.
- Cunjun Yu, Xiao Ma, Jiawei Ren, Haiyu Zhao, and Shuai Yi. Spatio-temporal graph transformer networks for pedestrian trajectory prediction. In *European Conference on Computer Vision*, pages 507–523. Springer, 2020.
- Shengyu Zhu, Ignavier Ng, and Zhitang Chen. Causal discovery with reinforcement learning. In *International Conference on Learning Representations*, 2019.
- Sirui Xie, Hehui Zheng, Chunxiao Liu, and Liang Lin. Snas: stochastic neural architecture search. In *International Conference on Learning Representations*, 2019.
- Wengong Jin, Regina Barzilay, and Tommi Jaakkola. Junction tree variational autoencoder for molecular graph generation. In *International Conference on Machine Learning*, pages 2323–2332. PMLR, 2018.
- Thomas Kipf, Ethan Fetaya, Kuan-Chieh Wang, Max Welling, and Richard Zemel. Neural relational inference for interacting systems. In *International Conference on Machine Learning*, pages 2688–2697. PMLR, 2018.
- Paul Erdős and Alfréd Rényi. On the evolution of random graphs. *Publ. Math. Inst. Hung. Acad. Sci.*, 5(1):17–60, 1960.
- Jiaxuan You, Rex Ying, Xiang Ren, William Hamilton, and Jure Leskovec. Graphrnn: Generating realistic graphs with deep auto-regressive models. In *International Conference on Machine Learning*, pages 5708–5717. PMLR, 2018.
- Namrata Anand and Po-Ssu Huang. Generative modeling for protein structures. In *Proceedings of the 32nd International Conference on Neural Information Processing Systems*, pages 7505–7516, 2018.
- Ashish Vaswani, Noam Shazeer, Niki Parmar, Jakob Uszkoreit, Llion Jones, Aidan N Gomez, Łukasz Kaiser, and Illia Polosukhin. Attention is all you need. In *Proceedings of the 31st International Conference on Neural Information Processing Systems*, pages 6000–6010, 2017.

- Yu Rong, Wenbing Huang, Tingyang Xu, and Junzhou Huang. Dropedge: Towards deep graph convolutional networks on node classification. In *International Conference on Learning Representations*, 2019.
- Luca Franceschi, Mathias Niepert, Massimiliano Pontil, and Xiao He. Learning discrete structures for graph neural networks. In *International conference on machine learning*, pages 1972–1982. PMLR, 2019.
- Maosen Li, Siheng Chen, Xu Chen, Ya Zhang, Yanfeng Wang, and Qi Tian. Actional-structural graph convolutional networks for skeleton-based action recognition. In *Proceedings of the IEEE/CVF Conference on Computer Vision and Pattern Recognition*, pages 3595–3603, 2019.
- Zhe Huang, Aamir Hasan, Kazuki Shin, Ruohua Li, and Katherine Driggs-Campbell. Long-term pedestrian trajectory prediction using mutable intention filter and warp lstm. *IEEE Robotics and Automation Letters*, 6(2):542–549, 2021.
- Eric Jang, Shixiang Gu, and Ben Poole. Categorical reparameterization with gumbel-softmax. In *International Conference on Learning Representations*, 2017.
- Chris J Maddison, Andriy Mnih, and Yee Whye Teh. The concrete distribution: A continuous relaxation of discrete random variables. In *International Conference on Learning Representations*, 2017.
- Stefano Pellegrini, Andreas Ess, Konrad Schindler, and Luc Van Gool. You’ll never walk alone: Modeling social behavior for multi-target tracking. In *Proceedings of the IEEE/CVF International Conference on Computer Vision*, pages 261–268, 2009.
- Alon Lerner, Yiorgos Chrysanthou, and Dani Lischinski. Crowds by example. In *Computer graphics forum*, volume 26, pages 655–664. Wiley Online Library, 2007.
- Diederik P Kingma and Jimmy Ba. Adam: A method for stochastic optimization. In *International Conference on Learning Representations*, volume 1412, 2015.